



## An investigation into the electrodeposition of AuCu-matrix particulate composites. Part II: Baths not containing free cyanide

B. BOZZINI<sup>1</sup>, G. GIOVANNELLI<sup>2</sup> and P.L. CAVALLOTTI<sup>2</sup>

<sup>1</sup>*INFM – Dipartimento di Ingegneria dell'Innovazione, Facoltà di Ingegneria, Università di Lecce, v. Arnesano, I-73100 Lecce, Italy*

<sup>2</sup>*Dipartimento di Chimica Fisica Applicata, Politecnico di Milano, v. Mancinelli 7, I-20131 Milano, Italy*

Received 5 July 1999; accepted in revised form 23 November 1999

*Key words:* electrodeposition of composites, electrodeposition of alloys, Au–Cu, B<sub>4</sub>C

### Abstract

In this paper we report on the electrodeposition of AuCu/B<sub>4</sub>C composites from acid baths with gold cyanocomplexes and no free cyanide. The electrochemical behaviour of the bath and the metallographic and crystalline structures of the electrodeposited alloys were studied with and without addition of particles. Electrochemical instabilities were previously observed for free-cyanide baths and their bearing on the structure of both pure matrix and composite electrodeposits were elucidated. No instabilities were observed in the alloy deposition from the acid baths containing complexed cyanide: compositionally and structurally homogeneous microstructures were obtained both with and without particle embedding.

### 1. Introduction

In a companion paper [1] we investigated the electrochemical and structural behaviour of AuCu/B<sub>4</sub>C codeposition baths containing Au<sup>+</sup> and Cu<sup>+</sup> cyanocomplexes and free cyanide, displaying cathodic passivation and the associated electrochemical and compositional instabilities. In the present paper we propose a similar system with EDTA as a complexing agent for Cu<sup>2+</sup> and without free cyanide. Such baths do not show electrochemical instabilities, the composition of the alloy is homogeneous and local compositional effects of particle addition are not observed.

### 2. Experimental details

#### 2.1. Analytical methods

Microscopic and structural work was carried out with SEM and XRD. Quantitative image analysis was performed as described in [2].

Electrochemical investigations on baths not containing particles were performed with potentiodynamic and galvanostatic measurements carried out with a computer-controlled galvanostat–potentiostat; an Ag/AgCl RE was connected to the cathodic surface via a Piontelli lateral channel probe [3]. These experiments were run in prismatic Pyrex cells with plane-parallel electrodes and magnetic stirring. Hydrodynamic conditions and current distribution were characterized [4]. The cathodic

material was polycrystalline Cu in the form of slabs; the cathodes were finished with a metallographic polish and were activated with sulphamic acid immediately before electrodeposition. The cathodically active surface (6.25 cm<sup>2</sup>) was defined with square PTFE windows. The anode was a platinized titanium expanded mesh electrode. Galvanostatic and potentiodynamic measurements on baths with and without dispersion of ceramic particles were carried out in the laboratory cell described in Section 2.2.

All the cathodic potentiodynamic experiments were run by scanning the cathodic potential from the immersion potential at a rate of 1 mV s<sup>-1</sup>. The behaviour of the cathodic kinetics was confirmed by means of replicated runs and with inverted ('return') potentiodynamic scans (not reported in the following, for brevity). As far as electrochemical measurements on the cell for composite plating are concerned, the measured cell potentials were corrected for ohmic drop and anodic overvoltage with suitable calibrations.

#### 2.2. Materials

An acidic EDTA Au–Cu electrodeposition bath was investigated; the composition and operating conditions are reported in Table 1. The ceramic material was B<sub>4</sub>C, the particles had an average diameter of 2.52 μm and a median diameter of 0.6 μm. The bath loading was 20 g dm<sup>-3</sup>.

A schematic top view of the laboratory cell for electrodeposition of composites is shown in Figure 1.

Table 1. Composition and operating conditions for the EDTA Au–Cu bath

Au (as $\text{KAu}(\text{CN})_2$ )	$7.5 \text{ g dm}^{-3}$
Cu (as $\text{CuO}$ )	$2.5 \text{ g dm}^{-3}$
EDTA	$11.5 \text{ g dm}^{-3}$ ([EDTA]:[CuO] = 1:1)
Citric acid	$40 \text{ g dm}^{-3}$
Ammonium citrate	$40 \text{ g dm}^{-3}$
T	$40 \text{ }^\circ\text{C}$
pH	5–7
c.d.	$10\text{--}20 \text{ mA cm}^{-2}$
Deposition rate <sup>‡</sup>	$32\text{--}37 \text{ } \mu\text{m h}^{-1}$
Cathodic efficiency <sup>‡</sup>	$\sim 73\%$

<sup>‡</sup> for  $18 \text{ mA cm}^{-2}$  with  $\text{B}_4\text{C}$   $20 \text{ g dm}^{-3}$

This cell consisted of a Pyrex cylinder of diameter  $D_C = 140 \text{ mm}$  and height  $100 \text{ mm}$  containing  $1 \text{ dm}^3$  of solution. Temperature control within  $\pm 0.5 \text{ }^\circ\text{C}$  was achieved by surrounding the cell with a thermostatic bath. The cell was equipped with two concentric cylindrical platinised Ti expanded mesh anodes  $A_1$  and  $A_2$  of diameters  $D_{A1} = 137.5 \text{ mm}$  and  $D_{A2} = 40 \text{ mm}$ , respectively. The outer anode  $A_1$  was fixed to the internal side of the Pyrex cell wall and the inner one to a central Pyrex shaft welded to the bottom of the Pyrex container.

The cathode C, of diameter  $d_C = 10 \text{ mm}$ , revolved around the axis of the cell with a revolution radius  $R_R = 450 \text{ mm}$ . The motion was achieved with a crank device driven by a stepping motor located above the cell. Electric connection was provided by a sliding contact. The rotation rate typically adopted was  $120 \text{ rpm}$ , under these conditions the Reynolds number was approximately 6000, corresponding to turbulent flow [5]. This kind of motion ensures optimal hydrodynamic conditions for particle incorporation. The cathodes were polycrystalline Cu cylinders. Prior to deposition they were metallographically polished and activated with sulphamic acid.

### 3. Results and discussion

#### 3.1. Electrochemical measurements

The bath shows a regular alloy deposition behaviour, with Au being the more readily deposited metal, in the

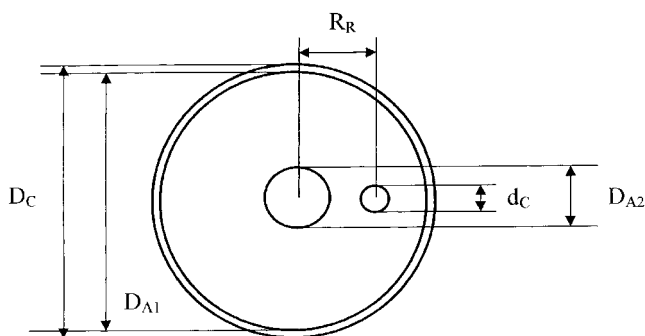


Fig. 1. Schematic top view of the laboratory cell for electrodeposition of composites (drawing not to scale).

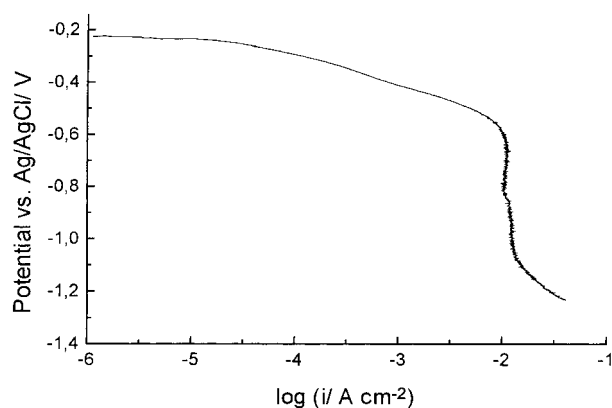


Fig. 2. Cathodic potentiodynamic curve for the acidic EDTA Au–Cu bath (pH 6,  $T = 40 \text{ }^\circ\text{C}$ , scanning rate  $1 \text{ mV s}^{-1}$ ).

current density (c.d.) and pH ranges considered. The potentiodynamic behaviour (Figure 2) is not appreciably affected by pH variations in the range 5–7 and does not show a sigmoidal behaviour. Addition of particles does not alter the potentiodynamic curve greatly, as indicated by the data of Table 2, where cathodic voltages are reported as measured in the laboratory cell (cell voltages corrected for anodic and ohmic contributions) for baths with and without dispersion of  $\text{B}_4\text{C}$ . Also the cathodic current efficiency (73% at  $18 \text{ mA cm}^{-2}$ ) is not measurably affected by the presence of particles in the bath.

#### 3.2. Electrodeposition experiments

Figure 3 shows a SEM cross sections of a codeposit obtained at c.d.  $15 \text{ mA cm}^{-2}$  with a dispersion of  $\text{B}_4\text{C}$ . The morphology of the layer is homogeneous for backscattered electron SEM. The Au content is 79 wt %.

Composition against c.d. curves for depositions with and without  $\text{B}_4\text{C}$  (Figure 4) show a positive correlation between c.d. and less noble metal content; this effect is more marked at the lower c.d. values. At high c.d. values ( $20 \text{ mA cm}^{-2}$ ) the alloy composition approaches the metal cation concentration ratio in the bath. Under these conditions compositional effects of particle additions are negligible. Inspection of the composition against c.d. curves shows that the presence of  $\text{B}_4\text{C}$

Table 2. Effects of particle addition to the cathodic overvoltage as a function of current density for the acidic bath (cell voltages corrected for anodic and ohmic effects)

$i/\text{mA cm}^{-2}$	$\eta$ vs Ag/AgCl/V no $\text{B}_4\text{C}$	$\eta$ vs Ag/AgCl/V $\text{B}_4\text{C}$ $20 \text{ g dm}^{-3}$
10	-1.72	-1.70
12	-1.75	-1.75
14	-1.82	-1.80
16	-1.98	-1.97
18	-2.22	-2.20
20	-2.38	-2.35

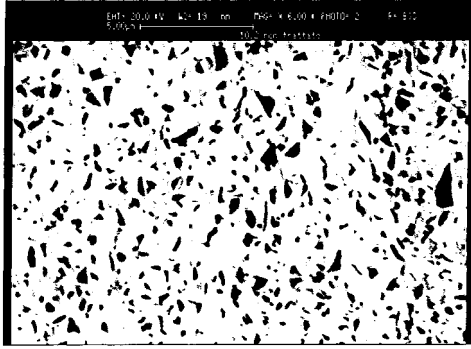


Fig. 3. SEM cross section of Au-Cu/B<sub>4</sub>C deposited from the acid EDTA bath (15 mA cm<sup>-2</sup>, B<sub>4</sub>C 20 g dm<sup>-3</sup>, Au 79 wt %).

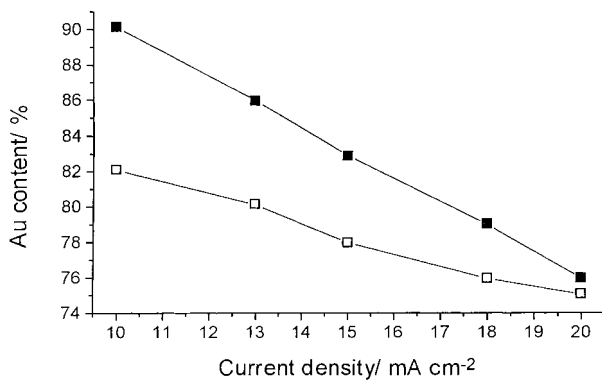


Fig. 4. Au contents in deposits from the acid EDTA Au-Cu bath with (20 g dm<sup>-3</sup>) (□) and without (■) B<sub>4</sub>C.

allows a given deposit composition to be reached for considerably lower c.d. values and, correspondingly lower cell voltages. This agrees with the above-reported observation that B<sub>4</sub>C additions do not alter cathodic polarization curves and cathodic current efficiency.

### 3.3. X-ray diffractographic studies

Typical diffractograms (Figure 5) for deposits of the same composition with and without particles show the formation of a solid solution. In both cases one FCC phase can be observed, with lattice parameters intermediate between those of Au and Cu. Compositional data from Végard's law (e.g., [6]) are in good agreement with the EDS results.

## 4. Conclusions

- (i) High free-cyanide cyanoalkaline baths have been reported [1] to display a sigmoidal potentiodynamic behaviour and, correspondingly, an unstable galvanodynamic behaviour. Metallographic cross sections of deposits obtained from such baths show a laminar structure with alternate Au-enriched and Au-depleted regions. This behaviour was explained by the absorption of cuprous complexes with a high CN<sup>-</sup> coordination number, which are not electroactive for low cathodic overvoltage values. This unstable behaviour is suppressed in baths containing Cu<sup>2+</sup>-EDTA complexes with just one electroactive species for Cu<sup>2+</sup>.
- (ii) Embedding of nonconductive particles in baths displaying both sigmoidal and non-sigmoidal potentiodynamic behaviour correlates with an increase of the content of the less noble alloying element. This phenomenon can be interpreted in terms of an increase in the average deposition c.d. due to cathodic screening effects brought about by the presence of the insulating particles. In alloy baths not displaying potentiodynamic sigmoidal behaviour (EDTA) this phenomenon is the only observed consequence of dispersing particles, while in baths

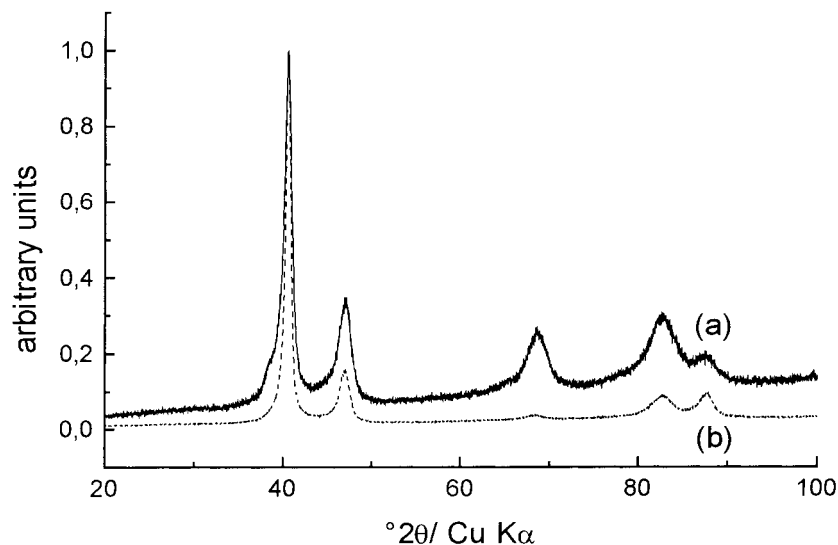


Fig. 5. X-ray diffractograms of deposits from acid EDTA Au-Cu bath: (a) without B<sub>4</sub>C (20 mA cm<sup>-2</sup>, Au 76 wt %) and (b) with B<sub>4</sub>C (20 g dm<sup>-3</sup>, 18 mA cm<sup>-2</sup>, Au weight 76%), showing solid-solution structures.

displaying unstable behaviour (cyanoalkaline solutions) in addition to this phenomenon, compositional heterogeneities are present.

- (iii) Compositional effects of the presence of particles are diminished by c.d. increases in baths not showing potentiodynamic sigmoidal behaviour. For higher c.d.s than the limiting c.d. values for the deposition of both metals, the composition of the deposited alloy approaches the ratio of metal cation concentrations of the bath. This phenomenon corresponds to the typical behaviour for alloy electrodeposition under diffusion control.

## References

1. B. Bozzini, G. Giovannelli and P.L. Cavallotti, *J. Appl. Electrochem.* **29** (1999) 685.
2. B. Bozzini, P.L. Cavallotti, G. Giovannelli, B. Brevaglieri and S. Natali, *Praktische Metallographie – Practical Metallography* **33** (1996) 130.
3. R. Piontelli, *Corrosion* **9** (1953) 115.
4. B. Bozzini, F. Pavan, G. Bollini and P.L. Cavallotti, *Trans. IMF* **75**(5) (1997) 175.
5. V.G. Levich, 'Physicochemical Hydrodynamics' (Prentice Hall, Englewood Cliffs, NJ, 1962), p. 34.
6. T.B. Massalski, in R.W. Cahn and P. Hassen (eds), 'Physical Metallurgy' (North Holland, Amsterdam, 1983), p. 178.